



Oleuropein aglycone in lipid bilayer membranes. A molecular dynamics study



Vicente Galiano^a, José Villalain^{b,*}

^a Physics and Computer Architecture Department, Spain

^b Molecular and Cellular Biology Institute, Universitas "Miguel Hernández", E-03202 Elche-Alicante, Spain

ARTICLE INFO

Article history:

Received 11 May 2015

Received in revised form 11 August 2015

Accepted 12 August 2015

Available online 14 August 2015

Keywords:

Oleuropein

Molecular dynamics

Membrane location

ABSTRACT

Olive oil has been recognized to possess many therapeutic applications. Its beneficial effects arise from many causes, but one of them lies on the presence of oleuropein aglycone (OA). OA presents a plethora of pharmacological beneficial properties. Although there is a great research going on the effect of polyphenols and their derivatives on different aspects of health, much less knowledge is available of the molecular basis of their beneficial effects. Due to the prominent hydrophobic character of OA and its high phospholipid/water partition coefficient, some of its possible effects on biological systems might be related to its capacity to interact with and locate into the membrane. In this work we have aimed to locate the molecule of OA in two membrane model systems, i.e., POPC/Chol and POPC/POPG/Chol. OA locates in between the hydrocarbon acyl chains of the phospholipids but its specific location and molecular interactions differ depending on the lipid system. OA is nearer to the membrane surface in the POPC/Chol system but it is located at a deeper position in the POPC/POPG/Chol system. Furthermore, OA seems to interact stronger with POPG than with POPC, implying the existence of specific interactions with negatively-charged phospholipids. Some of the biological effects of OA could be due to its preferential location in the membrane depending on the membrane lipid composition as well as the existence of specific interactions with specific phospholipids.

© 2015 Elsevier B.V. All rights reserved.

1. Introduction

Virgin olive oil contains a large amount of triacylglycerols as well as small quantities of other compounds such as fatty acids, phenols, pigments, sterols, tocopherols and many others [1,2]. The pharmacological properties of olive oil have been recognized to possess many therapeutic applications giving place to a healthy diet known as the Mediterranean diet [3]. The beneficial effects of the Mediterranean diet arises from many causes, and one of them lies on the increased contents of polyphenols and secoiridoids present in different food complements, including olive oil but also green tea and red wine. Phenols are found in all parts of the olive plant and oleuropein (OLE), a secoiridoid, together with its aglycone derivative, oleuropein aglycone (OA), is the most abundant polyphenols in *Oleaceae*, in particular *Olea Europaea* and represent the main phenolic oleosides found in virgin olive oil [1,3–6]. OLE and OA present a plethora of pharmacological beneficial properties, such as antioxidant, anti-inflammatory, anti-atherogenic, skin-protectant, anti-

cancer, antimicrobial and antiviral effects as well as having cardio- and neuro-protective roles [1,3,4,7–17]. Consequently, many experimental, clinical and epidemiological studies suggest that the consumption of phenolic-enriched foods reduces many chronic diseases [18,19]. Recently it has been shown that oleuropein aglycone (OA) presents anticancer activity related to the activation of anti-aging/cellular stress-like gene signatures, suppress epithelial-to-mesenchymal transition signaling cascade and suppress genes involved in the Warburg effect as well as protect against Alzheimer-associated neurodegeneration [3,6,8,10,11,20,21]. Interestingly, OA is more effective than OLE as an inhibitor of Tau fibrillization [22]. Although there is a great research ongoing on the effect of polyphenols and their derivatives on different aspects of health, much less knowledge is available of the molecular and cellular basis of their beneficial effects. These beneficial phenolic molecules can be envisaged more as nutraceuticals than drugs. Much information is needed in order to use them, not only from the biochemical and clinical point of view but also on their location and the specific interactions they might possess with other biomolecules.

OLE is an ester of 2-(3,4-dihydroxyphenyl)ethanol (hydroxytyrosol) and the glucosidic form of elenolic acid and some of its effects, similarly to other molecules, have been ascribed to its capacity to interact with biological membranes [1]. However, different studies have indicated that OLE locates either at a superficial position in the membrane or at its internal part, depending on membrane lipid composition [23–25]. Its

Abbreviations: Chol, cholesterol; OA, oleuropein aglycone; OLE, oleuropein; POPC, 1-palmitoyl-2-oleoyl-sn-glycero-3-phosphocholine; POPG, 1-palmitoyl-2-oleoyl-sn-glycero-3-phospho-(1'-rac-glycerol).

* Corresponding author at: Instituto de Biología Molecular y Celular, Universitas "Miguel Hernández", E-03202 Alicante, Spain.

E-mail address: jvillalain@umh.es (J. Villalain).

deglycosylation by beta-glucosidases present in different compartments of the plant or by intestinal bacteria gives rise to OA [26,27], a molecule that is more hydrophobic than OLE. The presence of the methoxycarbonyl group in OA favors its cyclic hemiacetalic form (Fig. 1) due to the conjugation of the ester group with the internal double bond [20]. Due to the prominent hydrophobic character of OA and its high phospholipid/water partition coefficient, some of its possible effects on biological systems might be related to its capacity to interact with and locate into the palisade structure of the membrane [25,28]. However, it should be taken into account that the partition coefficient of a molecule estimates its lipophilicity but does not give any clue about its location and orientation in the membrane. Furthermore, the interaction of the molecule with the membrane and its location inside it might change its physical properties and therefore modulate the interaction of the membranes with other biological molecules, which could account for its biological activities.

In this work we aim to discern the location and orientation of OA inserted in model membranes by atomistic molecular dynamics (MD). MD is a very useful methodology to probe the dynamics, interaction, structure and location of phospholipids in biological model membranes as well as different types of molecules inserted in them [29]. The fact that OA mode of action is most likely through membrane interaction, it seems reasonable to think that its mode of action might be at least partly attributable to its specific effect on the membrane structure, its specific interactions with particular lipid molecules and, last but not least, its location inside the membrane. For that goal, we have used two different types of model membranes, one composed of the zwitterionic phospholipid phosphatidylcholine (1-palmitoyl-2-oleoyl-sn-glycero-3-phosphocholine, POPC) and the other one containing both the zwitterionic phospholipid, POPC, and the negatively-charged phosphatidylglycerol (1-palmitoyl-2-oleoyl-sn-glycero-3-phospho-(1'-rac-glycerol), POPG). Our results support a superficial location of OA in the membrane and the existence of specific interactions with

specific phospholipids that could explain, at least in part, some of its biological effects.

2. Methods

2.1. Molecular dynamics simulation

Unrestrained all-atom molecular dynamics simulations were carried out using NAMD 2.9 [30] utilizing the CHARMM36 force field for the lipid molecules [31] and the CHARMM general force field for OA [32] obtained from http://mackerell.umaryland.edu/charmm_ff.shtml. The TIP3P model was used for water [33]. All simulations were carried out with a constant number of particles as an NPT ensemble at 1.0 atm and 310 K. The time step was 2 fs. Constant pressure was maintained by the Nosé–Hoover Langevin piston method [34,35]. Constant temperature was maintained by Langevin dynamics with a damping coefficient γ of 0.5 ps^{-1} . The standard particle mesh Ewald method was used with periodic boundary conditions to calculate the long-range electrostatic interaction of the systems. Non-bonded interactions were cut off after 12 Å with a smoothing function applied after 10 Å [36]. Prior to simulation and in order to remove unfavorable atomic contacts, the membrane model systems were previously equilibrated for 1 ns after 50,000 steps of minimization. The production trajectory of the lipid systems was calculated for 150 ns. All simulations were conducted under electrostatically neutral environment with an appropriate number of sodium ions.

2.2. Bilayer membrane model

We have used two different lipid bilayer models, one of them composed of POPC/Chol at a molar ratio of 7:1 and the other one composed of POPC/POPG/Chol at a molar ratio of 5:2:1. Each model comprised 128 lipid molecules (64 lipids in each leaflet) in a rectangular box. The POPC/Chol system was comprised by 16 molecules of cholesterol and

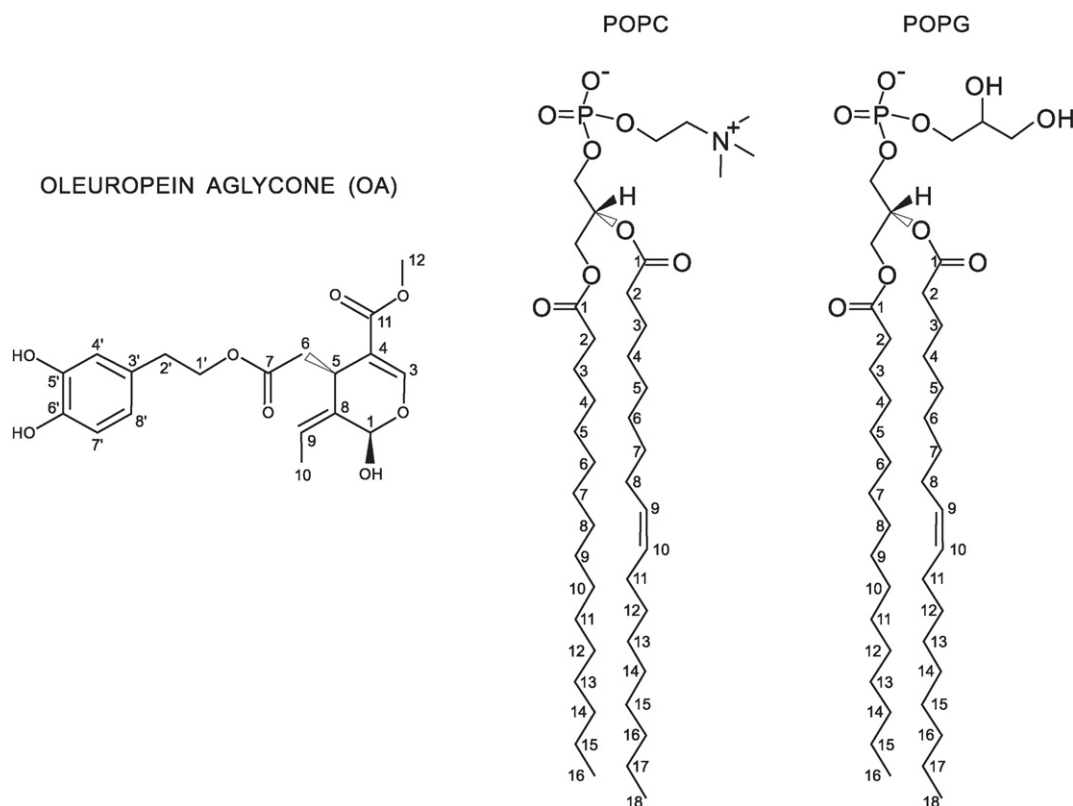


Fig. 1. Molecular structures of the hemiacetalic cyclic form of oleuropein aglycone (OA), 1-palmitoyl-2-oleoyl-sn-glycero-3-phosphocholine (POPC) and 1-palmitoyl-2-oleoyl-sn-glycero-3-phospho-(1'-rac-glycerol) (POPG). Numbering of particular atoms mentioned in the text is also given.

112 molecules of 1-palmitoyl-2-oleoyl-sn-glycero-3-phosphocholine (POPC) surrounded by 5780 molecules of water. The POPC/POPG/Chol system was comprised by 16 molecules of cholesterol, 80 molecules of POPC and 32 molecules of POPG surrounded by 5560 molecules of water. The phospholipid/cholesterol ratio chosen represents 12.5% of cholesterol in the sample. Cholesterol is an indispensable molecule for the organization and organization of the membrane and modifies the physico-chemical properties of the lipid bilayer. However, there are many different phospholipid/cholesterol ratios found in biological membranes, from less than 5% (ER, mitochondria) to more than 40% (erythrocyte), so that we have taken a compromise. In this way, the cholesterol content we have used does not affect largely the simulation time scale but better simulates a model biomembrane. The solvent-to-lipid ratio was ~45 for the POPC/Chol and ~43 for the POPC/POPG/Chol one, i.e., excess water [37]. Fig. 1 presents the structures and carbon numbering of the molecules considered in this study, OA, POPC and POPG. The bilayer lied in the xy plane and the bilayer normal was parallel to the z-axis. Initially the simulation box had the dimensions of 8.9 nm in the x- and y-directions and 8 nm in the z-direction. The height of the simulation box and the cross sectional area was allowed to vary independently of each other. Each water layer had an average dimension of 5.4 Å between membranes due to periodic boundary conditions. OA was generated and minimized using Discovery Studio 4.0 software (Accelrys Inc., San Diego, USA). As it is well known, phosphatidylcholine is the dominant lipid species in biological membranes, cholesterol is omnipresent in many types of membranes giving them unique biophysical properties and phosphatidylglycerol provides negative charge at the membrane surface [38]. Since we have used POPC and POPG, the palmitoyl chain located in the sn-1 position is completely saturated, whereas the oleoyl chain located in the sn-2 position contains a cis double bond between the C9 and C10 carbons (see Fig. 1 for acyl chain numbering). The presence of the oleoyl chain in the sn-2 position increases the overall mobility of the hydrocarbon chains of the phospholipids and hence fluidity in the xy plane of the membrane. The lipid membrane models, including POPC, POPG, cholesterol and OA, were prepared using the Charmm-Gui web server (<http://www.charmm-gui.org>, [39]). ParamChem (<https://cgenff.paramchem.org>, [32]) was used to obtain the CHARMM General Force Field (CGenFF) compatible stream file of OA which contained the optimized parameter and topology data of the molecule (for the optimization guide see <http://mackerell.umaryland.edu/~kenno/cgenff/>). The automatic PSF generation plugin for VMD [40] utilized the OA stream file data to obtain the psf and pdb files of OA required by NAMD to build the complete system. Since OA has a highly hydrophobic character, a high phospholipid/water partition coefficient and it is known to insert into the membrane, at the beginning of the simulation the OA molecule was embedded at the center of the lipid bilayer in order to quickly reach convergence. This configuration was specifically chosen so that the simulation did not extend excessively in the time scale [41].

2.3. Analysis

The surface of the membrane was defined by the layer of the phosphate atoms of the phospholipid headgroups and were oriented parallel to the xy plane. Bilayer thickness was defined as the average distance between the phospholipid phosphorus atoms of the opposing leaflets, whereas the center of the bilayer, $z = 0$, was defined by the center-of-mass of the phosphate atoms of the phospholipid molecules. The center of mass z-distance of the OA molecule relative to the center of the bilayer was used to study its spatial distribution in the membrane. The OA membrane relative orientation was measured by the angle defined by the z-axis and the vector defined by carbons C4 and C4' of the molecule of OA (see Fig. 1 for numbering). The analysis was performed over the whole MD simulation unless stated otherwise. VMD [40] and Pymol [42] were used for visualization and analysis. SCD order parameters, membrane thickness, molecular areas, center-of-mass and molecule

tilt were obtained using VMD Membrapugin [43] whereas the mass density profiles were obtained using the VMD Density Profile Tool plugin [44].

3. Results and discussion

As an indicator of the equilibration of the bilayer we have used the time variation of the area per lipid and to assess the adequacy of the simulation methodology we have obtained its average value [45,46]. The time traces of the area per molecule, i.e., POPC, POPG, cholesterol and OA, corresponding to the $z +$ and $z -$ leaflets for the system POPC/Chol are shown in Fig. 2A and B, respectively, whereas those corresponding to the $z +$ and $z -$ leaflets for the system POPC/POPG/Chol are shown in Fig. 2C and D, respectively. As expected, no significant changes were found in the general bilayer properties in these diluted systems, i.e., systems having only one molecule of OA. The data show that for both systems studied in this work, POPC/Chol and POPC/POPG/Chol, phospholipids and cholesterol were equilibrated early on the course of the simulations, either at the $z +$ or at the $z -$ bilayer leaflets, indicating that the systems reached a steady state after 10 ns of simulation. At the end of the simulation, the mean area of POPC and Chol was 59–60 Å² and 39–36 Å², respectively, in both membrane systems whereas it was 59 Å² for POPG in the POPC/POPG/Chol system, in agreement with previously reported data [47]. However, the behavior of the molecular area of OA was different from those of the phospholipids and cholesterol. In the first place, the OA molecular area presented a great variation along the whole simulation time in both membrane systems (compare the area variation of OA with that of the phospholipids, Fig. 4A and C). This is due to the structure of the OA molecule and its location and disposition in the membrane (see below). In the second place, the OA molecular area was equilibrated with its surroundings at about 10 ns for the system POPC/POPG/Chol (Fig. 2C) but for the system POPC/Chol the OA molecular area was equilibrated with its surroundings much later, i.e., at about 115 ns (see Fig. 2A). The inserts in Fig. 2A and C show the area histograms for OA for the last 5 ps of the simulation for the systems POPC/Chol and POPC/POPG/Chol, respectively. It can be observed that the mean area for OA in the POPC/Chol system is about 100 Å² whereas is about 85 Å² in the POPC/POPG/Chol system. In a similarly way to the behavior of the area vs. time trend commented above, membrane thickness, measured as the average distance between the phosphate atoms of opposite leaflets, was held relatively constant after 13 and 10 ns for the systems POPC/Chol and POPC/POPG/Chol, respectively, indicating again a rapid equilibration of both systems (Fig. 2E and F).

The initial and final configurations for both POPC/Chol and POPC/POPG/Chol membrane model systems are shown in Fig. 3. As commented above and at the start of the simulation, the OA molecule was located in the middle of the palisade structure of the bilayer at the same coordinates for both systems (Fig. 3A and B for POPC/Chol and POPC/POPG/Chol systems, respectively). At the end of the simulation OA locates near the surface in vicinity to the phospholipid headgroups for the POPC/Chol system (Fig. 3C). However, in the POPC/POPG/Chol system OA, although moves slightly towards the membrane interface, remains buried in between the hydrocarbon chains of the phospholipids of the $z +$ leaflet (Fig. 3D). It is clear from this pictures that OA locates below the phospholipid headgroups but relatively far from the bilayer center.

This behavior is clearly observed in the time variation of the center-of-mass of OA for both membrane model systems (Fig. 4A and B for the systems containing POPC/Chol and POPC/POPG/Chol, respectively). For the system POPC/Chol and at about 25 ns, OA equilibrates in a position which remains relatively similar to that found at the end of the simulation, i.e., 150 ns (Fig. 4A). The time needed by OA to reach the equilibrium position in the POPC/POPG/Chol system is similar, being also about 25 ns, remaining in that position until the end of the simulation (Fig. 4B). However, the difference in final location in both systems is

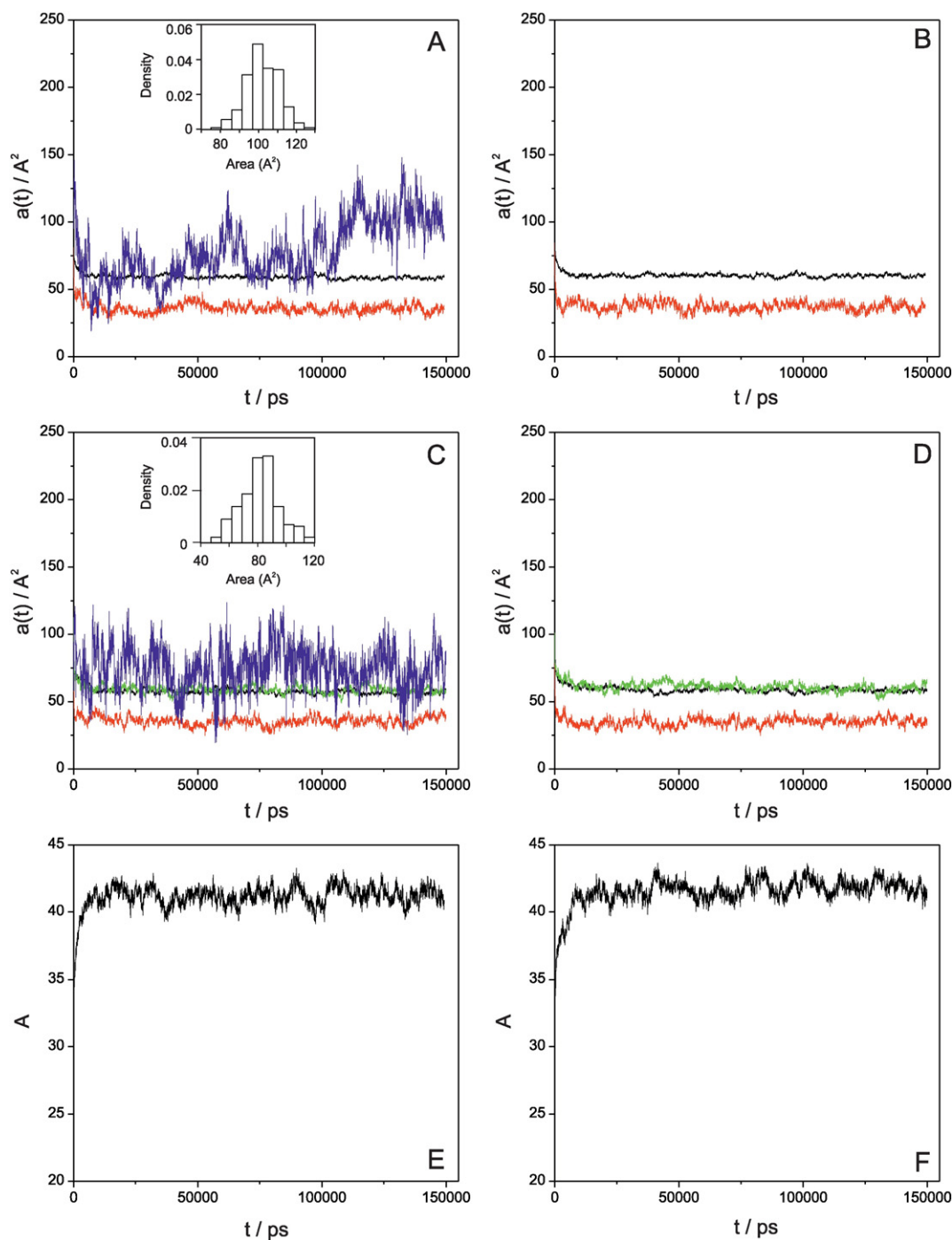


Fig. 2. Time variation of the (A–D) molecular areas of each species in the $z+$ (A, C) and $z-$ (B, D) leaflets of the bilayer and (E, F) membrane thickness for membrane model systems composed of (A, B, E) POPC/Chol/OA and (C, D, F) POPC/POPG/Chol/OA. In plots A–D black, green, red, and blue stand for POPC, POPG, Chol and OA, respectively. Inserts in (A) and (B) show the area histograms for OA for the last 5 ps in each membrane system.

clearly observed in Fig. 4A and B. Whereas the final average relative location of OA in the POPC/Chol system is about 17.5 Å, the final average relative location of OA in the POPC/POPG/Chol system is about 6.8 Å. It is important to note also the great deviation in OA location, since for the last 1 ns the location of OA in the POPC/Chol system oscillates between 15 and 19 Å whereas in the POPC/POPG/Chol system oscillates between 5.5 and 9 Å (Fig. 4A and B).

Mass density profiles were calculated for all components of both systems studied in this work, POPC/Chol (Fig. 4C) and POPC/POPG/Chol (Fig. 4D). As observed in Fig. 4C, OA lies on average at a depth slightly lower than the phosphate groups of both phospholipids, POPC and POPG, at the same level as the OH group of cholesterol. This is in contrast

to the location of OA in the POPC/POPG/Chol system, since its location is similar to that of the cholesterol tail (approximately between atoms C21 and C27 of cholesterol) as observed in Fig. 4D. It is interesting to note that the density profile of the phosphate atoms located in the $z+$ leaflet in the POPC/POPG/Chol system is rather asymmetric when compared to the density profile of the phosphate atoms located in the $z-$ leaflet (Fig. 4D). This data would imply the existence of at least two different populations of phosphate atoms regarding to their relative location in the membrane.

Fig. 4E shows the mass density profile of the phosphate atoms of POPC and POPG phospholipids in the POPC/POPG/Chol system where it can be observed the existence of subtle but significant differences.

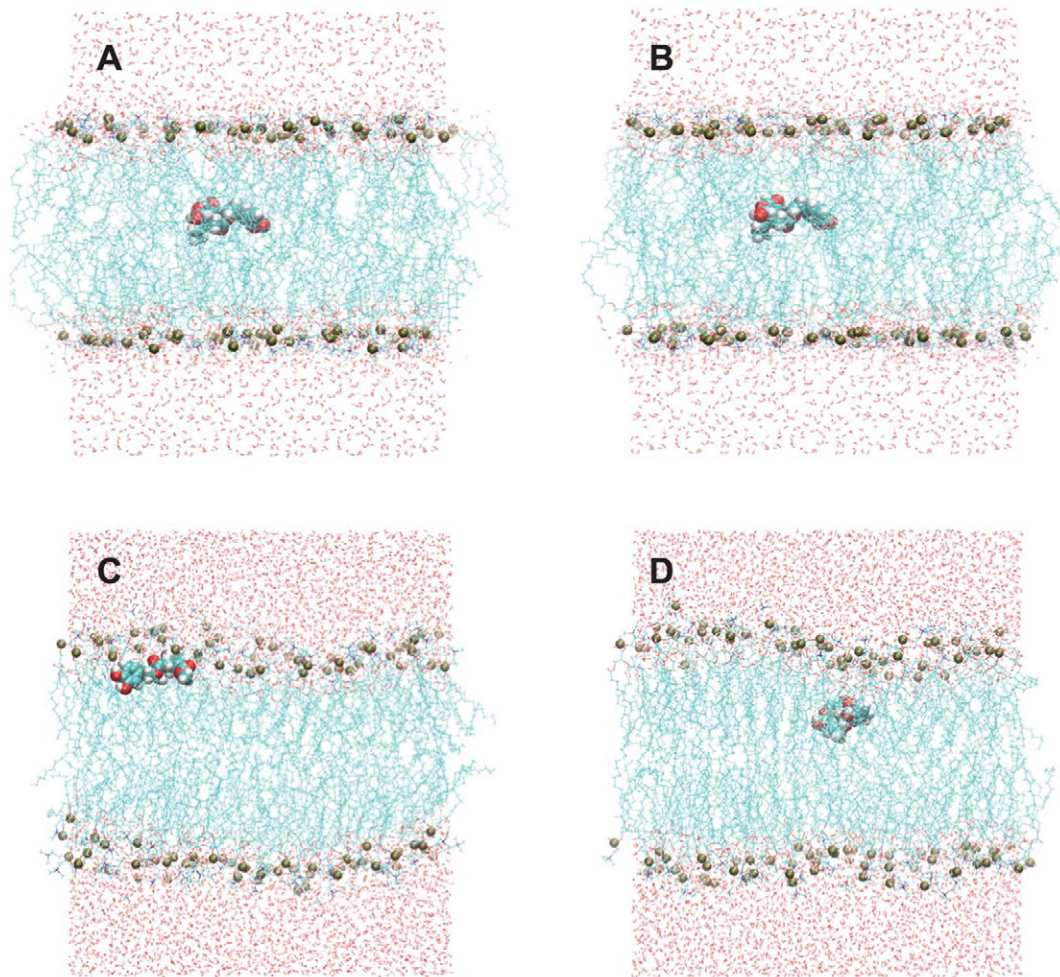


Fig. 3. Initial ($t = 0$) and final ($t = 150$ ps) snapshots of (A, C) POPC/Chol and (B, D) POPC/POPG/Chol membrane model systems. The phospholipid and water molecules are shown in light blue and red, respectively. The OA molecule and the phosphate atoms are depicted in VDW drawing style.

The density profile maxima for the phosphate atoms of POPC and POPG in the $z -$ leaflet are 20.8 and 20.5 Å, respectively, but the maxima for the phosphate atoms of POPC and POPG in the $z +$ leaflet are 21.9 and 20.1 Å, respectively. The difference in the maxima is therefore 0.3 and 0.8 Å for the $z -$ and the $z +$ leaflets, respectively, which would indicate that the positioning of the phosphate atoms of POPC and POPG are different in the membrane, being lower for the phosphate atoms of POPG than those of POPC. Furthermore, significant differences can be observed for the half bandwidth of the density profiles in both leaflets. The half bandwidth of the density profile corresponding to the POPC phosphate atoms in the $z -$ leaflet is 5.5 Å whereas it is 4.9 Å for the phosphate atoms of POPG. In the case of the $z +$ leaflet, the half bandwidth of the density profile corresponding to the POPC phosphate atoms is 7 Å whereas it is 7.3 Å for the phosphate atoms of POPG. Therefore, the density profiles corresponding to the phosphate atoms of both phospholipid types are broader in the $z +$ leaflet than in the $z -$ one, going from 5.5 to 7 Å in the case of the phosphate atoms of POPC (a difference of 1.5 Å) and from 4.9 to 7.3 in the case of the phosphate atoms of POPG (a difference of 2.4 Å). This data would imply that OA affects to a higher extend the molecules of POPG than those of POPC (see below).

The orientation of OA in the membrane was studied considering the angle formed by the molecular axis defined by the vector joining OA carbons 4 and 4' with the bilayer normal (Fig. 5A and B for the POPC/Chol and POPC/POPG/Chol systems, respectively). As observed in Fig. 5A, which corresponds to OA in the POPC/Chol system, there was a great

variation in angle along the simulation time, ranging from a minimum value of about 5° at the beginning of the simulation time and a maximum one of 176° in the middle. At the end of the simulation, the variation was much lower, with an average angle of about 95° with a deviation of $\pm 15^\circ$ (Fig. 5A, insert). For the system POPC/POPG/Chol, the deviation at the beginning of the simulation was much higher than in the middle and end of it as observed in Fig. 5B. The values ranged from a minimum value of about 14° and a maximum of 166° . The general variation was much lower than that observed for OA in the POPC/Chol system. At the end of the simulation, the average angle was about 80° having a deviation of $\pm 10^\circ$ (Fig. 5B, insert). We have also analyzed the distance between carbons 4 and 4' of OA along the simulation and the data is represented in Fig. 5C and D for the systems POPC/Chol and POPC/POPG/Chol, respectively. Similarly to the angle variation commented above, the distance between carbons 4 and 4' varied greatly along the simulation time. For OA in POPC/Chol the values ranged from 4.9 Å to 9.8 Å (Fig. 5C), whereas for OA in POPC/POPG/Chol the values ranged from 3.7 Å to 10.2 Å (Fig. 5D). At the end of the simulation, the average distance was 8.8 Å for OA in POPC/Chol and 8.3 Å in POPC/POPG/Chol. Fig. 5E and F show the final structures of OA in the POPC/Chol and POPC/POPG/Chol systems, respectively. It can be observed that their disposition in the membrane is not completely different, since as commented above, the difference in the angles are about 15° ; however, their overall conformation is different, at least if we compare the relative disposition of the rings in the molecule.

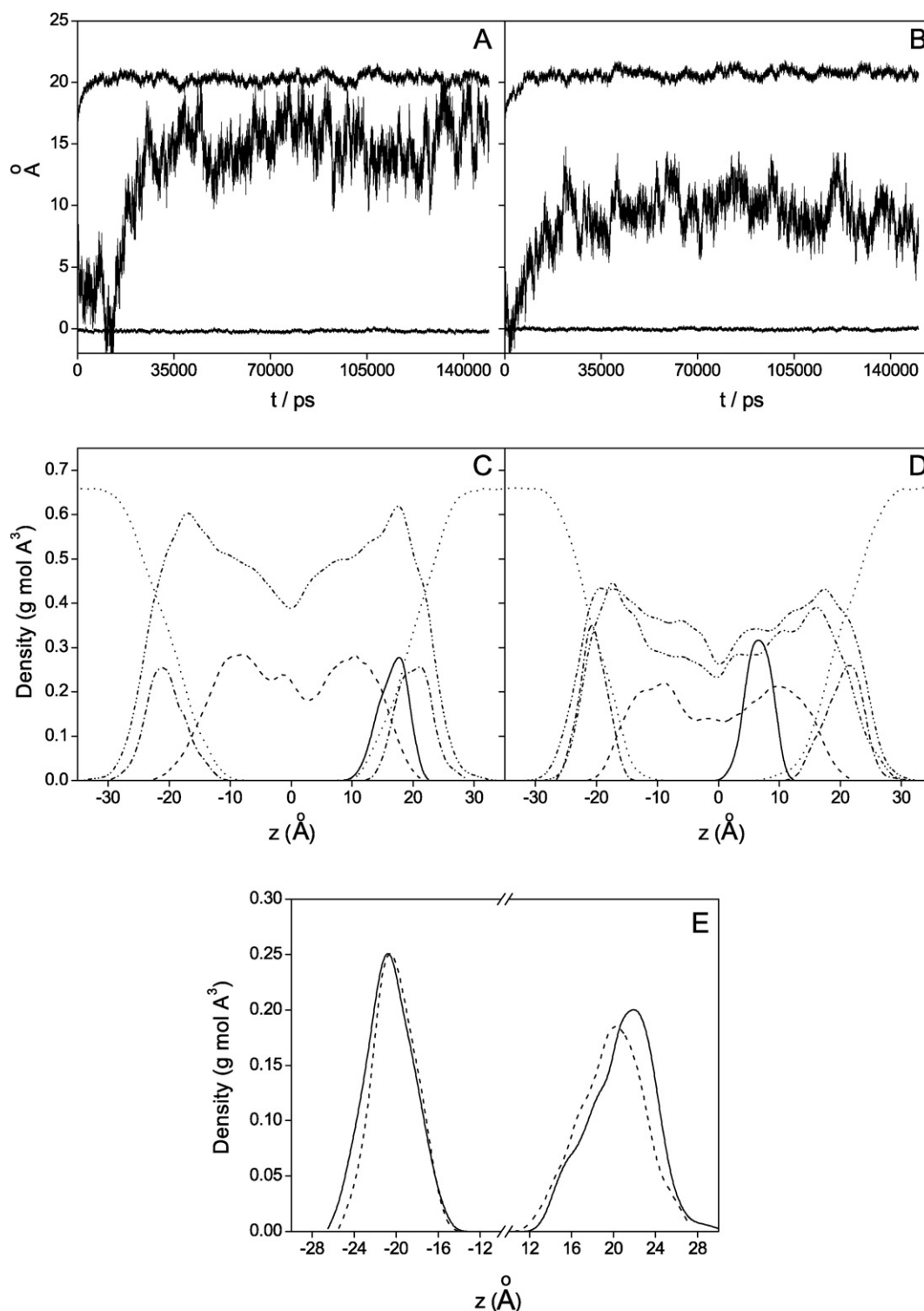


Fig. 4. Time variation of the OA center-of-mass for the membrane systems containing (A) POPC/Chol and (B) POPC/POPG/Chol, respectively. The average center-of-mass of OA, the $z+$ leaflet phosphate atoms and the $z+$ and $z-$ leaflets phosphate atoms are visible. Mass density profiles for the last 1 ns of the simulation for OA (—, multiplied by 10), water (····), POPC and POPG (— · — · —, POPG multiplied by 2), cholesterol (—, multiplied by 3) and phospholipid phosphate atoms (— · — · —, multiplied by 3) for the (C) POPC/Chol and (D) POPC/POPG/Chol (B, D) systems. The enlargement of the mass density profile of the phosphate groups of POPC (—) and POPG (—, multiplied by 2) for the POPC/POPG/Chol system is shown in (E).

Until now, we have described the location, disposition and orientation of OA in both model membrane systems, POPC/Chol and POPC/POPG/Chol. However, membrane order is affected by OA and we have investigated the effect of the presence of the molecule of OA on the nearest phospholipid acyl chains. As noted above, OA barely affects membrane thickness and slightly the average location of POPC and

POPG phosphate atoms. However, membrane order is evident in the deuterium order parameter $-S_{CD}$ of the hydrocarbon acyl chains of the phospholipids. $-S_{CD}$ can vary between 0.5, i.e., full order along the normal bilayer, and -0.25 , i.e., full order along the bilayer plane [48]. When $-S_{CD}$ is equal to 0 it indicates isotropic orientation. Therefore, we have calculated the $-S_{CD}$ values for both saturated and

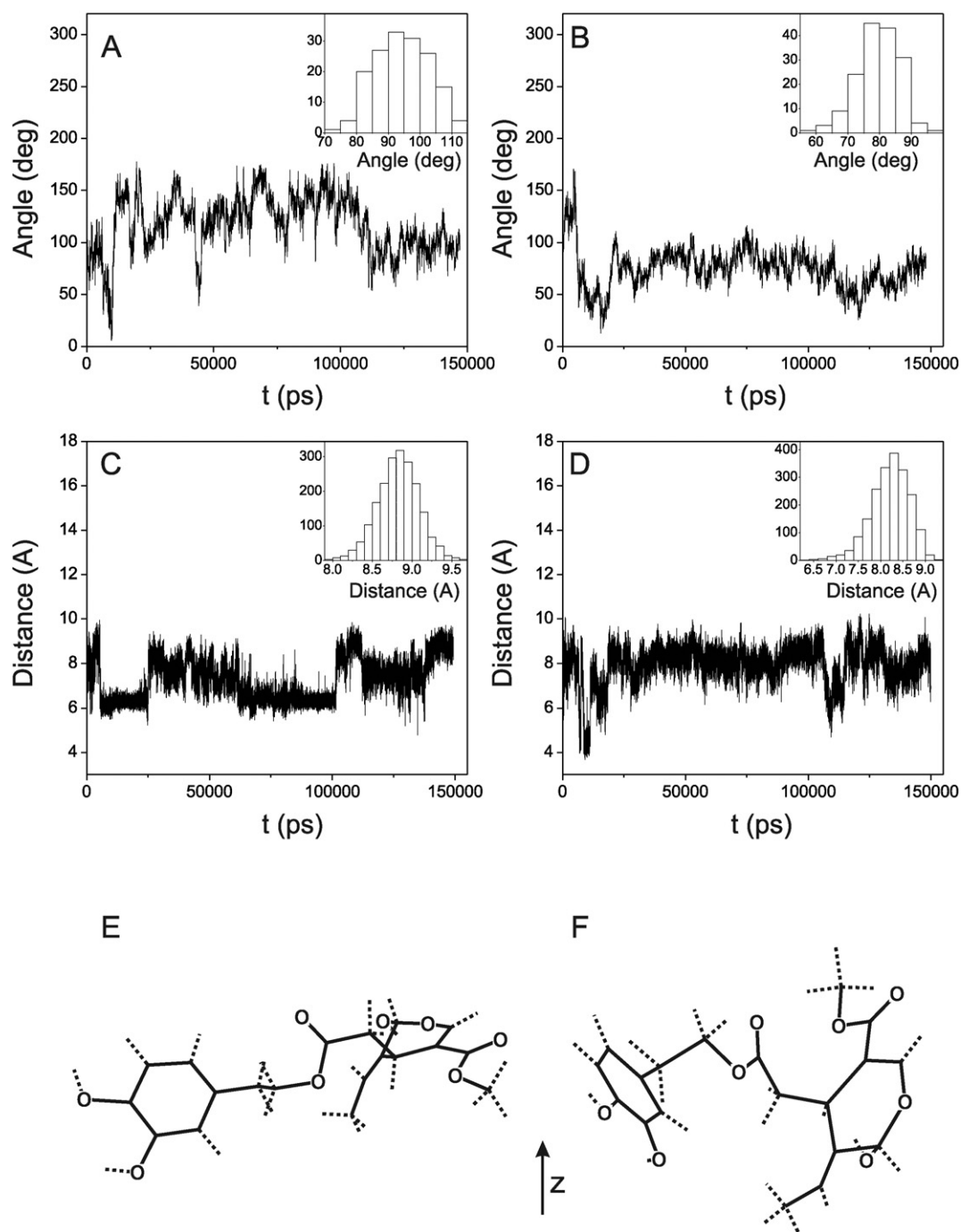


Fig. 5. Time variation of the angle defined by the vector joining carbons 4–4' of OA and the membrane z axis (A, B) and time variation of the distance between carbons 4 and 4' of OA (C, D) for the POPC/Chol (A, C) and POPC/POPG/Chol (B, D) systems. The inserts show the histograms of the angle and distance variation for the last 2 ns of the simulation. The final structures of OA in (E) POPC/Chol and (F) POPC/POPG/Chol are shown. Dotted lines represent CH/OH bonds.

unsaturated acyl chains of POPC and POPG in both model membrane systems and the results are shown in Fig. 6. The average $-S_{CD}$ values for the sn-1 and sn-2 acyl chains of POPC for the POPC/Chol system in both leaflets, z+ and z-, are relatively similar (Fig. 4A and B, respectively), in agreement with the profiles observed earlier for experimental and simulated data [31,49,50]. However, it should be taken into account that there are 56 molecules of POPC and 8 molecules of cholesterol per leaflet in the system but only one molecule of OA (see above). Because of that, we have calculated the $-S_{CD}$ values of the POPC molecules that are within 7 Å of the molecule of OA as shown in Fig. 6A and B for the sn-1 and sn-2 acyl chains, respectively. It is evident from the figures

that the presence of OA gives place to small but significant effects on carbons 4–12 of the acyl chains of POPC. They can be understood by noting that OA has two rings in a relatively rigid structure, the molecule does not completely span the leaflet of the bilayer and its location is coincidental with carbons 4–12 of the acyl chains (see Fig. 4).

The average $-S_{CD}$ values for the sn-1 acyl chains of POPC and POPG in the POPC/POPG/Chol system are shown in Fig. 4C and E, respectively, whereas the average $-S_{CD}$ values for the sn-2 acyl chains of POPC and POPG are shown in Fig. 4D and F, respectively. Although the POPC/POPG/Chol system has one molecule of OA plus 40 molecules of POPC, 16 molecules of POPG and 8 molecules of Chol in each leaflet, there

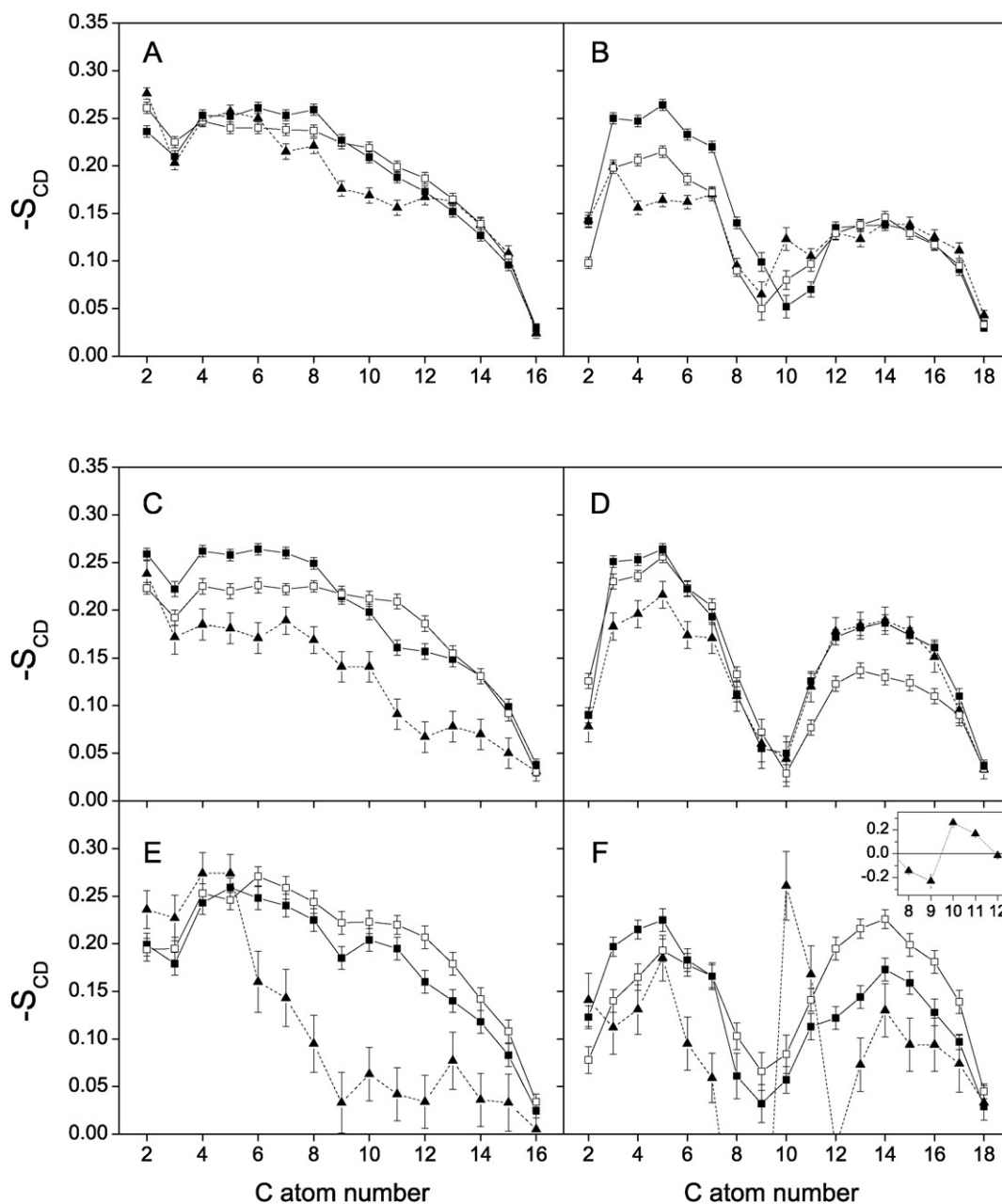


Fig. 6. Deuterium order parameter $-S_{CD}$ calculated for the sn-1 (A, C, E) and sn-2 (B, D, F) acyl chains of POPC (A–D) and POPG (E, F) for the membrane model systems composed of (A, B) POPC/Chol and (C–F) POPC/POPG/Chol. The average $-S_{CD}$ parameters for the z+ (■) and z- (□) bilayer leaflets and the $-S_{CD}$ parameters for the lipid acyl chains within 7 Å of the molecule of OA (▲) are shown. The analysis was carried out for the last 1 ns of simulation.

are noticeable differences between the $-S_{CD}$ values of POPC and POPG. These differences might reflect the long range effects of the specific location of OA in the membrane. More interesting is the differential effect observed for both the sn-1 and sn-2 chains of those molecules of POPC and POPG near OA. OA decreases the $-S_{CD}$ values of all carbons pertaining to the acyl sn-1 chains of both POPC and POPG near it, but the effect is significantly higher for POPG than for POPC (compare Fig. 6C and D). The effect is different but more noteworthy when the $-S_{CD}$ values pertaining to the sn-2 chains of POPC and POPG are compared (Fig. 6D and F). The presence of OA lowered the $-S_{CD}$ values of the carbons 2–7 pertaining to the sn-2 chain of POPC but no effect was visible on the other ones (Fig. 6D). The effect was more dramatic for the sn-2 chain of POPG when compared to the average $-S_{CD}$ values, since OA lowered the $-S_{CD}$ values of all carbons of the sn-2 acyl chain of POPG except carbons 10 and 11 (Fig. 6F). More interestingly, the $-S_{CD}$ values of carbons 8, 9 and 12 were negative (-0.14 , -0.23 and

-0.014 , respectively) whereas the $-S_{CD}$ values of carbons 10 and 11 were 0.26 and 0.17, respectively. These data would imply that OA reduced the acyl chain order parameter of the sn-2 acyl chain of POPG but locally increased the order parameter of the unsaturated carbons of the phospholipid.

4. Conclusions

A number of literature studies have suggested that oleuropein aglycon (OA) resides in the membrane and its mode of action might be attributable to its effect on the membrane as a whole and/or specific lipid molecules inserted in them. However, a definite assessment of its location is still lacking. This work aimed to locate the molecule of oleuropein aglycon (OA) in the membrane and discern, if possible, the specific interactions of the molecule with membrane lipids using molecular dynamics simulations. For that aim, we have used two membrane

model systems, i.e., POPC/Chol and POPC/POPG/Chol. Although there is the evident limitation of simulating a single molecule inserted in the membrane, our simulation provides a detailed clue on the nature of interactions and location of OA in the membrane. Moreover, we have used a simulation time of 150 ns, which should be enough to permit the equilibration of all the molecules of the systems and therefore obtain meaningful conclusions about them. One of the main conclusion we can obtain from this study is that OA locates in between the hydrocarbon acyl chains of the phospholipids. However, its specific location and molecular interactions differ depending on the lipid system. In the POPC/Chol system, OA is nearer to the membrane surface than to the middle of the palisade structure of the membrane; on the contrary, OA tends to be located in a deeper position, nearer to the center of the membrane in the POPC/POPG/Chol system. This difference in OA location depending on membrane system is reinforced by the effect of OA in the order parameters of the phospholipids, which is stronger on POPG than on POPC. These data would suggest the existence of specific interactions with negatively-charged phospholipids rather than zwitterionic ones. Finally, and regarding the biological activity of OA, it should be noted that it tends to be preferentially located in a specific location in the membrane where its spatial concentration should be higher than inferred from the specific OA contents in available foods, whereby increasing its *in vivo* biological activities.

Declarations of interest

None to declare.

Acknowledgments

The research conducted in this work was partially funded by grant BFU2013-43198-P (Ministerio de Economía y Competitividad, Spain) to J.V. NAMD was developed by the Theoretical and Computational Biophysics Group in the Beckman Institute for Advanced Science and Technology at the University of Illinois at Urbana-Champaign.

References

- [1] S. Lopez, B. Bermudez, S. Montserrat-de la Paz, S. Jaramillo, L.M. Varela, A. Ortega-Gomez, R. Abia, F.J. Muriana, Membrane composition and dynamics: a target of bioactive virgin olive oil constituents, *Biochim. Biophys. Acta* 1838 (2014) 1638–1656.
- [2] A. Bendini, L. Cerretani, A. Carrasco-Pancorbo, A.M. Gomez-Caravaca, A. Segura-Carretero, A. Fernandez-Gutierrez, G. Lercker, Phenolic molecules in virgin olive oils: a survey of their sensory properties, health effects, antioxidant activity and analytical methods. An overview of the last decade, *Molecules* 12 (2007) 1679–1719.
- [3] J.A. Menendez, J. Joven, G. Aragones, E. Barrajon-Catalan, R. Beltran-Debon, I. Borrás-Linares, J. Camps, B. Corominas-Faja, S. Cufi, S. Fernandez-Arroyo, A. Garcia-Heredia, A. Hernandez-Aguilera, M. Herranz-Lopez, C. Jimenez-Sanchez, E. Lopez-Bonet, J. Lozano-Sanchez, F. Luciano-Mateo, B. Martin-Castillo, V. Martin-Paredero, A. Perez-Sanchez, C. Oliveras-Ferraras, M. Riera-Borrull, E. Rodriguez-Gallego, R. Quirantes-Pine, A. Rull, L. Tomas-Menor, A. Vazquez-Martin, C. Alonso-Villaverde, V. Micol, A. Segura-Carretero, Xenohormetic and anti-aging activity of secoiridoid polyphenols present in extra virgin olive oil: a new family of gerosuppressant agents, *Cell Cycle* 12 (2013) 555–578.
- [4] S.H. Omar, Oleuropein in olive and its pharmacological effects, *Sci. Pharm.* 78 (2010) 133–154.
- [5] C.C. Tangney, M.J. Kwasny, H. Li, R.S. Wilson, D.A. Evans, M.C. Morris, Adherence to a Mediterranean-type dietary pattern and cognitive decline in a community population, *Am. J. Clin. Nutr.* 93 (2011) 601–607.
- [6] A. Vazquez-Martin, S. Fernandez-Arroyo, S. Cufi, C. Oliveras-Ferraras, J. Lozano-Sanchez, L. Vellon, V. Micol, J. Joven, A. Segura-Carretero, J.A. Menendez, Phenolic secoiridoids in extra virgin olive oil impede fibrogenic and oncogenic epithelial-to-mesenchymal transition: extra virgin olive oil as a source of novel antiaging phytochemicals, *Rejuvenation Res.* 15 (2012) 3–21.
- [7] S.H. Omar, Cardioprotective and neuroprotective roles of oleuropein in olive, *Saudi Pharm. J.* 18 (2010) 111–121.
- [8] F. Casamenti, C. Grossi, S. Rigacci, D. Pantano, I. Luccarini, M. Stefani, Oleuropein Aglycone, A possible drug against degenerative conditions. *In vivo* evidence of its effectiveness against Alzheimer's disease, *J. Alzheimers Dis.* 45 (2015) 679–688.
- [9] I. Luccarini, C. Grossi, S. Rigacci, E. Coppi, A.M. Pugliese, D. Pantano, G. la Marca, T. Ed Dami, A. Berti, M. Stefani, F. Casamenti, Oleuropein aglycone protects against pyroglutamylation-3 amyloid-ss toxicity: biochemical, epigenetic and functional correlates, *Neurobiol. Aging* 36 (2015) 648–663.
- [10] I. Luccarini, T. Ed Dami, C. Grossi, S. Rigacci, M. Stefani, F. Casamenti, Oleuropein aglycone counteracts Abeta42 toxicity in the rat brain, *Neurosci. Lett.* 558 (2014) 67–72.
- [11] C. Grossi, S. Rigacci, S. Ambrosini, T. Ed Dami, I. Luccarini, C. Traini, P. Failli, A. Berti, F. Casamenti, M. Stefani, The polyphenol oleuropein aglycone protects TgCRND8 mice against Ass plaque pathology, *PLoS One* 8 (2013) e71702.
- [12] L. Diomedea, S. Rigacci, M. Romeo, M. Stefani, M. Salmona, Oleuropein aglycone protects transgenic *C. elegans* strains expressing Abeta42 by reducing plaque load and motor deficit, *PLoS One* 8 (2013) e58893.
- [13] Z. Janahmadi, A.A. Nekoeian, A.R. Moaref, M. Emamghoreishi, Oleuropein offers cardioprotection in rats with acute myocardial infarction, *Cardiovasc. Toxicol.* 15 (2015) 61–68.
- [14] S.H. Choi, H.B. Joo, S.J. Lee, H.Y. Choi, J.H. Park, S.H. Baek, S.M. Kwon, Oleuropein prevents angiotensin II-mediated: human vascular progenitor cell depletion, *Int. J. Cardiol.* 181C (2014) 160–165.
- [15] S. De Marino, C. Festa, F. Zollo, A. Nini, L. Antenucci, G. Raimo, M. Iorizzi, Antioxidant activity and chemical components as potential anticancer agents in the olive leaf (*Olea europaea* L. cv Leccino.) decoction, *Anti Cancer Agents Med. Chem.* 14 (2014) 1376–1385.
- [16] C. Muscoli, F. Lauro, C. Dagostino, S. Ilari, L.A. Giancotti, M. Gliozzi, N. Costa, C. Carresi, V. Musolino, F. Casale, D. Ventrice, M. Oliverio, E. Palma, S. Nistico, A. Procopio, M. Rizzo, V. Mollace, Olea Europea-derived phenolic products attenuate antinociceptive morphine tolerance: an innovative strategic approach to treat cancer pain, *J. Biol. Regul. Homeost. Agents* 28 (2014) 105–116.
- [17] B. Barbaro, G. Toietta, R. Maggio, M. Arciello, M. Tarocchi, A. Galli, C. Balsano, Effects of the olive-derived polyphenol oleuropein on human health, *Int. J. Mol. Sci.* 15 (2014) 18508–18524.
- [18] J.P.E. Spencer, A. Crozier, Flavonoids and related compounds: bioavailability and function, CRC Press, Boca Raton, 2012.
- [19] C.G. Fraga, Plant phenolics and human health: biochemistry, nutrition, and pharmacology, Wiley, Hoboken, NJ, 2010.
- [20] B. Corominas-Faja, E. Santangelo, E. Cuyas, V. Micol, J. Joven, X. Ariza, A. Segura-Carretero, J. Garcia, J.A. Menendez, Computer-aided discovery of biological activity spectra for anti-aging and anti-cancer olive oil oleuropeins, *Aging* 6 (2014) 731–741.
- [21] A. Daccache, C. Lion, N. Sibille, M. Gerard, C. Slomianny, G. Lippens, P. Cotelle, Oleuropein and derivatives from olives as Tau aggregation inhibitors, *Neurochem. Int.* 58 (2011) 700–707.
- [22] M. Kostomoiri, A. Fragkouli, M. Sagnou, L.A. Skaltsounis, M. Pelecanou, E.C. Tsilibary, A.K. Tzinia, Oleuropein, an anti-oxidant polyphenol constituent of olive promotes alpha-secretase cleavage of the amyloid precursor protein (AbetaPP), *Cell. Mol. Neurobiol.* 33 (2013) 147–154.
- [23] F. Castelli, D. Trombetta, A. Tomaino, F. Bonina, G. Romeo, N. Uccella, A. Saija, Dipalmitoylphosphatidylcholine/linoleic acid mixed unilamellar vesicles as model membranes for studies on novel free-radical scavengers, *J. Pharmacol. Toxicol. Methods* 37 (1997) 135–141.
- [24] F. Paiva-Martins, M.H. Gordon, P. Gameiro, Activity and location of olive oil phenolic antioxidants in liposomes, *Chem. Phys. Lipids* 124 (2003) 23–36.
- [25] N. Caturla, L. Perez-Fons, A. Estepa, V. Micol, Differential effects of oleuropein, a biophenol from *Olea europaea*, on anionic and zwitterionic phospholipid model membranes, *Chem. Phys. Lipids* 137 (2005) 2–17.
- [26] K. Konno, C. Hirayama, H. Yasui, M. Nakamura, Enzymatic activation of oleuropein: a protein crosslinker used as a chemical defense in the privet tree, *Proc. Natl. Acad. Sci. U. S. A.* 96 (1999) 9159–9164.
- [27] M. de Bock, E.B. Thorstensen, J.G. Derraik, H.V. Henderson, P.L. Hofman, W.S. Cutfield, Human absorption and metabolism of oleuropein and hydroxytyrosol ingested as olive (*Olea europaea* L.) leaf extract, *Mol. Nutr. Food Res.* 57 (2013) 2079–2085.
- [28] P.S. Rodis, V.T. Karathanos, A. Mantzavinou, Partitioning of olive oil antioxidants between oil and water phases, *J. Agric. Food Chem.* 50 (2002) 596–601.
- [29] H.I. Ingolfsson, M.N. Melo, F.J. van Eerden, C. Amarez, C.A. Lopez, T.A. Wassenaar, X. Periole, A.H. de Vries, D.P. Tieleman, S.J. Marrink, Lipid organization of the plasma membrane, *J. Am. Chem. Soc.* 136 (2014) 14554–14559.
- [30] J.C. Phillips, R. Braun, W. Wang, J. Gumbart, E. Tajkhorshid, E. Villa, C. Chipot, R.D. Skeel, L. Kale, K. Schulten, Scalable molecular dynamics with NAMD, *J. Comput. Chem.* 26 (2005) 1781–1802.
- [31] J.B. Klauda, R.M. Venable, J.A. Freites, J.W. O'Connor, D.J. Tobias, C. Mondragon-Ramirez, I. Vorobyov, A.D. MacKerell Jr., R.W. Pastor, Update of the CHARMM all-atom additive force field for lipids: validation on six lipid types, *J. Phys. Chem. B* 114 (2010) 7830–7843.
- [32] K. Vanommeslaeghe, E. Hatcher, C. Acharya, S. Kundu, S. Zhong, J. Shim, E. Darian, O. Guvench, P. Lopes, I. Vorobyov, A.D. MacKerell Jr., CHARMM general force field: a force field for drug-like molecules compatible with the CHARMM all-atom additive biological force fields, *J. Comput. Chem.* 31 (2010) 671–690.
- [33] M. Ozu, H.A. Alvarez, A.N. McCarthy, J.R. Grigera, O. Chara, Molecular dynamics of water in the neighborhood of aquaporins, *Eur. Biophys. J.* 42 (2013) 223–239.
- [34] S.E. Feller, Y. Zhang, R.W.J. Pastor, Constant pressure molecular dynamics simulation: the Langevin piston method, *J. Chem. Phys.* 103 (1995) 4613–4621.
- [35] G.J. Martyna, D.J. Tobias, M.L. Klein, Constant pressure molecular dynamics algorithms, *J. Chem. Phys.* 101 (1994) 4177–4189.
- [36] M. Patra, M. Karttunen, M.T. Hyvonen, E. Falck, P. Lindqvist, I. Vattulainen, Molecular dynamics simulations of lipid bilayers: major artifacts due to truncating electrostatic interactions, *Biophys. J.* 84 (2003) 3636–3645.
- [37] K. Murzyn, T. Rog, G. Jezierski, Y. Takaoka, M. Paskeniewicz-Gierula, Effects of phospholipid unsaturation on the membrane/water interface: a molecular simulation study, *Biophys. J.* 81 (2001) 170–183.

- [38] G. van Meer, D.R. Voelker, G.W. Feigenson, Membrane lipids: where they are and how they behave, *Nat. Rev. Mol. Cell Biol.* 9 (2008) 112–124.
- [39] E.L. Wu, X. Cheng, S. Jo, H. Rui, K.C. Song, E.M. Davila-Contreras, Y. Qi, J. Lee, V. Monje-Galvan, R.M. Venable, J.B. Klauda, W. Im, CHARMM-GUI Membrane Builder toward realistic biological membrane simulations, *J. Comput. Chem.* 35 (2014) 1997–2004.
- [40] W. Humphrey, A. Dalke, K. Schulten, VMD: visual molecular dynamics, *J. Mol. Graph.* 14 (1996) 33–38 27–38.
- [41] P. Kosinova, K. Berka, M. Wykes, M. Otyepka, P. Trouillas, Positioning of antioxidant quercetin and its metabolites in lipid bilayer membranes: implication for their lipid-peroxidation inhibition, *J. Phys. Chem. B* 116 (2012) 1309–1318.
- [42] The Pymol Molecular Graphics System, version 1.7.4, Schrödinger, LLC.
- [43] R. Guixa-Gonzalez, I. Rodriguez-Espigares, J.M. Ramirez-Anguaita, P. Carrio-Gaspar, H. Martinez-Seara, T. Giorgino, J. Selent, MEMBPLUGIN: studying membrane complexity in VMD, *Bioinformatics* 30 (2014) 1478–1480.
- [44] T. Giorgino, Computing 1-D atomic densities in macromolecular simulations: the Density Profile Tool for VMD, *Comput. Phys. Commun.* 185 (2014) 317–322.
- [45] C. Kandt, W.L. Ash, D.P. Tieleman, Setting up and running molecular dynamics simulations of membrane proteins, *Methods* 41 (2007) 475–488.
- [46] C. Anézo, A.H. de Vries, H.-D. Höltje, D.P. Tieleman, S.-J. Marrink, Methodological issues in lipid bilayers simulations, *J. Phys. Chem. B* 107 (2003) 9424–9433.
- [47] X. Zhuang, J.R. Makover, W. Im, J.B. Klauda, A systematic molecular dynamics simulation study of temperature dependent bilayer structural properties, *Biochim. Biophys. Acta* 1838 (2014) 2520–2529.
- [48] D.P. Tieleman, S.J. Marrink, H.J. Berendsen, A computer perspective of membranes: molecular dynamics studies of lipid bilayer systems, *Biochim. Biophys. Acta* 1331 (1997) 235–270.
- [49] H.H. Tsai, J.B. Lee, H.S. Li, T.Y. Hou, W.Y. Chu, P.C. Shen, Y.Y. Chen, C.J. Tan, J.C. Hu, C.C. Chiu, Geometrical effects of phospholipid olefinic bonds on the structure and dynamics of membranes: A molecular dynamics study, *Biochim. Biophys. Acta* 1848 (2015) 1234–1247.
- [50] R.A. Bockmann, A. Hac, T. Heimburg, H. Grubmüller, Effect of sodium chloride on a lipid bilayer, *Biophys. J.* 85 (2003) 1647–1655.